

1 *Full title:* Formation of virus-like particles from human cell lines exclusively expressing
2 Influenza neuraminidase.

3

4 *Running title:* Influenza NA alone can form virus like particles.

5

6 *Authors:* Jimmy C.C. Lai¹, Wallace W.L. Chan¹, François Kien¹, John M. Nicholls², J.S. Malik
7 Peiris^{1,3} and Jean-Michel Garcia^{1,*}.

8

9 ¹ HKU-Pasteur Research Centre, Hong Kong SAR, China

10 ² Department of Pathology, The University of Hong Kong, Hong Kong SAR, China

11 ³ Department of Microbiology, The University of Hong Kong, Hong Kong SAR, China

12

13 * *Corresponding author:* Dr JM Garcia, HKU-Pasteur Research Centre, Dexter H.C. Man

14 Building, 8 Sassoon Road, Pokfulam, Hong Kong SAR. Phone: (852) 2816-8460. Fax: (852)

15 2872-5782. E-mail: jmgarcia@hku.hk.

16

17 *Text:* **5230** words;

18 *Summary:* **112** words;

19 *Figures:* **6**

20 *Tables:* **0**.

21

22 **Summary:**

23 The minimal viral requirements for the generation of influenza virus like particle (VLP)
24 assembly and budding was reassessed. Using neuraminidase from the H5N1 and H1N1
25 subtypes, it was found that the expression of neuraminidase (NA) alone was sufficient to
26 generate and release VLPs. Biochemical and functional characterization of the NA containing
27 VLPs demonstrated that they were morphologically similar to influenza virions. The NA
28 oligomerization was comparable to that of the live virus, and the enzymatic activity, while not
29 required for the release of NA-VLP, was preserved. Together, these findings indicate that NA
30 plays a key role in virus budding and morphogenesis and demonstrates that NA-VLPs
31 represent a useful tool in influenza research.

32

33

34 **Introduction**

35 Influenza A viruses are lipid enveloped members of the *Orthomyxoviridae* family.
36 They contain 8 negative-sense, single-stranded RNA segments encoding 10 viral proteins.
37 Influenza virions are pleomorphic although generally their shape is roughly spherical with a
38 diameter around <150 nm. However, larger [100-400 nm] influenza virions are also
39 generated, as are filamentous forms (Fujiyoshi *et al.*, 1994).

40

41 Influenza viruses derive their lipid envelope by budding from the plasma membrane of
42 the infected cells and progeny virions are normally not found inside the host cell. Therefore
43 assembly and budding are the final, but essential steps in the virus life cycle. M1 matrix
44 protein is the most abundant protein in the influenza virion and plays a critical role in both
45 virus assembly and budding (reviewed in Nayak *et al.*, 2009). M1 affects virus assembly by
46 interacting with the core viral ribonucleocapsid (vRNP) and cytoplasmic tail of
47 transmembrane proteins, forming a bridge between the two layers, as well as recruiting the
48 internal viral proteins and vRNA to the plasma membrane in a cooperative manner (Noda *et al.*
49 *et al.*, 2006). In addition, M1 interacts with the lipid bilayer producing an outward bending of the

50 membrane and this has been postulated to be the major driving force of influenza budding
51 since cells expressing M1 protein alone assemble into virus-like particles (VLPs) (Gómez-
52 Puertas *et al.*, 2000; Latham & Galaeza, 2001).

53

54 Haemagglutinin (HA) and neuraminidase (NA) are the two major surface
55 glycoproteins in the influenza viral membrane. HA binds to sialic acid receptors on the cell
56 surface and mediates the fusion process (Matrosovich *et al.*, 2006); whereas NA cleaves the
57 terminal sialic acids from the cell surface glycans to facilitate release of the progeny virus
58 from the host cell and prevent aggregation of virus particles (Bucher & Palese, 1975; Air &
59 Laver, 1989). NA is also essential in the initial stage of virus infection by enhancing HA-
60 mediated fusion (Su *et al.*, 2009), helping the virus to penetrate the mucin barrier protecting
61 the airway epithelium (Matrosovich *et al.*, 2004) and promoting virus entry (Ohuchi *et al.*,
62 2006). Studies of mutant influenza viruses have previously shown that the cytoplasmic tails
63 of HA and NA contribute to control virus assembly (Zhang *et al.*, 2000) and virus morphology
64 (Jin *et al.*, 1997). The specific role of HA and NA in virus budding is controversial. COS-1
65 cells expressing HA alone did not give rise to virus like particles (VLP) production (Gómez-
66 Puertas *et al.*, 2000), however assembly and budding of a NA-deficient virus mutant could be
67 rescued with exogenous bacterial NA to the level of wild-type virus (Liu *et al.*, 1995). These
68 studies suggested that the presence of both viral proteins was not essential for virus budding.
69 Nevertheless, studies of cells expressing recombinant viral proteins from an H3N2 virus
70 demonstrated that both HA and NA were involved in the budding process (Chen *et al.*, 2007).

71

72 In this study, using a plasmid-driven VLP production system in human embryonic
73 kidney (HEK-293T) cells, we looked at the minimal viral requirements for influenza virus
74 assembly and budding. We showed that both H5 HA and N1 NA can be the driving forces for
75 virus budding, whereas M1 only had a limited contribution. In addition, we demonstrated that
76 expression of NA alone could lead to the budding of particles. The influenza VLPs with NA
77 (NA-VLPs) were morphologically similar to influenza virions and had an intact sialidase

78 enzymatic activity. Comparable results in generating NA VLPs were found with NA from both
79 seasonal and pandemic H1N1 and avian H5N1 viruses.

80

81 **Results**

82 **Determination of minimal viral requirement for VLP formation and release.** In
83 order to determine which viral structural protein(s) is/are essential for VLP-formation and
84 release, HEK-293T cells were transfected with plasmids encoding for H5N1 proteins HA, NA
85 and M1 singly, or in combination. Protein composition of the VLPs released into the culture
86 medium was analyzed by western blotting (Fig.1a) and budding of VLPs from the transfected
87 cells was visualized by transmission electron microscopy (Fig. 2). None of the transfections
88 affected the protein expression system as indicated by analysis of the glyceraldehyde 3-
89 phosphate dehydrogenase (GAPDH) housekeeping protein expression. Co-transfection of
90 genes coding for different viral proteins had a minimal impact on individual expression level
91 as shown in cell lysates (Fig. 1a). The expression of the HA, NA and M1 in the cytosol
92 appeared to be comparable. Release was quantified by densitometric analysis of the
93 Western blots and expressed as a percentage of overall production (cumulative both from
94 lysates and in supernatant). VLPs were not detected by western blot from the culture
95 medium of cells expressing HA alone unless exogenous bacterial NA was added (Fig. 1a,
96 lanes 1 vs. 2), suggesting that VLPs budding from HA-expressing cells could not be released
97 without exogenous NA as confirmed by VLP aggregation on the cell surface in TEM (Fig. 2a
98 vs. 2c). When M1 was expressed alone, a small amount of the protein was detected in the
99 supernatant and no significant change was observed by addition of exogenous NA (Fig. 1a,
100 lanes 4 & 5). However, we were not able to find VLP structures from cells expressing M1
101 alone (Fig. 2e) When HA and M1 were co-expressed, VLPs were released into the
102 supernatant only in the presence of exogenous bacterial NA (Fig. 1a, lanes 7 & 8) with an
103 increase of HA and M1 content when compared to their single-expression. Interestingly,
104 release of both HA and M1 was significantly enhanced by the co-expression of NA (Fig. 1a,
105 lanes 3, 6 & 9). Also, VLPs containing NA were easily detected from the cells expressing NA

106 exclusively (Fig. 1a, lane 10) and could be widely observed by TEM (Fig. 2d & 2f). These
107 results confirmed the requirement of the NA enzymatic activity for the HA-containing VLP
108 release, but also suggested a role of NA in VLP budding. Comparison of protein expression
109 in the cell lysates as well as in the supernatant of infected or HA/NA/M1 transfected cells
110 showed that HA and NA had similar expression levels (Fig. 1b), however the amount of M1
111 released with the budding VLPs in the supernatant was approximately half of that found in
112 virus infected cells. This was compatible with previous reports that M1 requires interaction
113 with other viral proteins, such as the structural proteins HA/NA (Wang et al., 2010), as well
114 as with viral RNPs which are absent from VLPs. Using TEM, the VLPs were pleomorphic
115 with spherical or filamentous forms (Fig. 2b & 2f), similar to influenza virions.

116

117 **Physical and functional characterization of NA-VLPs produced in cells**
118 **expressing influenza virus NA alone.** NA from the H5N1 subtype and from seasonal H1N1
119 and pandemic H1N1 subtypes were included in this study. Culture medium of cells
120 expressing the NA protein alone was harvested for detection of released particles. FLAG-
121 tagged NAs were used to allow the detection with anti-FLAG antibodies of the protein from
122 different viral origins at the same antibody binding affinity. No difference of VLP formation
123 efficiency was observed between tagged and non-tagged NA (data not shown). Furthermore,
124 similar particles were seen by TEM for all three subtypes we studied (Supplementary data
125 S1). Sucrose gradient (20-60 %) centrifugation analysis demonstrated the presence of NA-
126 VLPs in the intermediate pellet fractions between 30-50 % sucrose (Fig. 3 b-d), which was
127 similar to the result observed with influenza A/WSN/33(H1N1) virions (Fig. 3a). In contrast,
128 purified NA proteins were only present in lighter fractions (~20 % sucrose) of the gradient
129 (Fig. 3e). In addition, NA proteins either purified or on the VLP surface or from the virus were
130 functionally active as shown using a neuraminidase activity assay (Fig. 3f). The apparent
131 shift of one fraction towards a higher concentration of sucrose for the virus versus the VLP
132 was probably due to the presence of nucleic acid in the virus (RNPs) decreasing slightly their
133 buoyancy.

134

135 Kinetic analysis of the NA-VLP production showed that it was continuous over at least
136 60 hours post-transfection with continuous accumulation of the NA-VLP in the supernatant
137 (Fig. 4a) when using NA from both pandemic H1N1 or from H5N1. Cleavage of caspase-3
138 was not detected in all time-points indicating there was no evidence of apoptosis (Fig. 4b).
139 Electron micrographs of transfected cells also failed to manifest features of apoptosis during
140 the course of the experiment.

141

142 We found that sole expression of NA (from H5N1) was sufficient to promote release of
143 NA-VLP (Fig. 5). A mutation of NA in position 262 (E to D) which abrogated the sialidase
144 activity as well as treatment with Oseltamivir (sialidase inhibitor) failed to affect VLP
145 formation. As expected, co-expression of HA (H5 from H5N1) increased the release of NA
146 probably by the formation of heterochimeric VLP (HA/NA-VLP), but release of HA-containing
147 VLP was then dependent on sialidase activity.

148

149 Immunoblotting analysis of VLPs showed that the NAs on the particle surface were in
150 multimeric form, including the monomer (~55 kDa), dimer (~110 kDa), trimer (~165 kDa) and
151 tetramer (~220 kDa) (Fig. 6). Multimeric NA complexes on the VLPs were denatured into
152 monomer by heating in SDS loading buffer with chaotropic agent (urea) or reducing agent
153 (DTT) (lanes 1 to 3). Upon pre-treatment of DTSSP before the denaturing step, multimeric
154 NA complexes were protected from SDS and urea, and partially from DTT (lanes 4 to 6).
155 Similar multimeric NA complexes were detected in the H1N1 virions but the detection failed
156 in the samples pre-treated with DTSSP (lanes 7 & 8), probably due to the inability of the
157 antibody to recognize cross-linked antigens. Samples from highly pathogenic H5N1 virus
158 could not be analyzed as protocols for inactivating the infectivity of the highly pathogenic
159 virus H5N1 so that these preparations could be taken out of bio-safety level-3 containment
160 for further analysis compromises oligomer integrity.

161

162 Desialylation of cell surface sialic acids in cells expressing NA was then studied by
163 lectin binding (Supplementary data S2). A weak SNA binding was observed in HEK-293T
164 cells, indicating low level of α -2,6 linked sialic acid on the 293T cells, and this disappeared in
165 cells expressing any of the NAs studied. Similar loss of cell-surface sialic acids was seen in
166 NA VLP expressing A549 or MDCK cells which express more α -2,6 sialic acid (data not
167 shown). MAA binding confirmed the presence of α -2,3 linked sialic acid on mock transfected
168 293T cells and this was significantly decreased in NA-expressing cells. Cleavage of sialic
169 acids by sialidase is expected to expose the underlying Gal-GalNAc and this was
170 demonstrated by the increased binding of PNA to NA-expressing cells.

171

172 **Discussion**

173 Influenza assembly, budding and release are the last but important steps in the
174 replication cycle. VLP production assays using different systems have been developed to
175 determine the viral proteins involved in the virus budding (Gómez-Puertas *et al.*, 2000;
176 Latham & Galaeza, 2001; Neumann *et al.*, 2000). Here we investigated the minimal viral
177 components required for assembly and budding of H5N1 influenza virus using a plasmid-
178 driven VLPs formation system similar to that described in a previous study on H3N2 virus
179 (Chen *et al.*, 2007).

180

181 Previous findings about the major viral proteins responsible for the virus budding have
182 been contradictory. It was suggested that M1 plays the major role in driving virus budding
183 from the cellular membrane (Gómez-Puertas *et al.*, 2000), whereas Chen and his colleagues
184 found that M1 is not essential for the process but that HA and NA were necessary (Chen *et al.*,
185 2007). A recent publication (Wang *et al.*, 2010) confirmed that M1 by itself fails to form
186 virus-like particles, probably due to a lack of membrane-targeting signal and therefore
187 requires the interaction with other viral proteins to be incorporated in the budding virions. In
188 our study, although small amounts of M1 were released from the cells expressing M1 alone,
189 no budding particle was observed by electron microscopy (Fig. 2e). A similar finding was

190 recently reported in which it was suggested that M1 was only nonspecifically secreted into
191 the supernatant rather than released in the form of VLP (Tscherne et al., 2010). Nevertheless,
192 co-expression of M1 increased the level of both HA and NA incorporated into the VLPs
193 (compare Fig. 1a, lanes 2 & 8; lanes 6 & 10), suggesting that M1 helps the virus budding,
194 probably by pushing the inner side of the cellular membrane.

195

196 VLP formation in cells transfected with HA alone or HA/M1 was completely dependent
197 on the addition of exogenous NA. In the absence of exogenous NA, HA-containing VLPs
198 were aggregated on the cell surface and not released into the medium (Fig. 1 & 2).
199 Exogenous NA cleaved the cell surface sialic acids allowing the VLPs to be released,
200 therefore both HA and M1 became detectable in the medium. These results suggested that
201 the expression of HA could provide a driving force to trigger the production of VLP, although
202 exogenous NA was necessary for the release of the particles.

203

204 Previously it has been suggested that NA was important for virus morphogenesis.
205 Studies using influenza virus lacking cytoplasmic tails of HA or NA (HA⁻/NA⁻) demonstrated
206 that NA⁻ virus particles had an elongated morphology but not HA⁻ virus (Jin *et al.*, 1997).
207 Introduction of mutations in both the transmembrane and cytoplasmic domains of NA
208 confirmed that NA is critical to control the virus shape, size and titer (Barman *et al.*,
209 2004). Studies of mutant virus containing a large internal deletion in NA gene have shown
210 they can assemble and bud similarly to wild-type virus (Liu *et al.*, 1995). However, our data
211 has shown for the first time that expression of NA alone in HEK-293T cells could provide a
212 driving force for the formation of extracellular NA-containing particles and this finding was
213 seen with NA from different influenza viruses of the N1 subtype and demonstrated in at least
214 two additional human cell-lines (A549 and HeLa, data not shown). It is also important to note
215 that the release of M1 and HA was greatly enhanced by the co-expression with NA to a level
216 which was not acquired by high concentration of exogenous NA, indicating that NA is likely to
217 be a major force in driving virus budding. However, whereas Chen et al. (2007) reported that

218 only small amounts of NA were released when this glycoprotein was expressed on its own,
219 our data showed that a large amount of NA was released. This discrepancy is probably due
220 to the difference in influenza virus subtype used in the two studies (N2 in Chen et al., versus
221 N1 here). In fact we did observe that N2 subtype NA was expressed to much lower level than
222 N1 and that N1 from human seasonal H1N1 was expressed less than the highly pathogenic
223 avian H5N1 (Supplementary data S3).

224

225 Furthermore, using a potent sialidase inhibitor and a point mutation (E262D) in NA
226 that inactivates the catalytic site of the sialidase (Huang et al., 2008), we could show that
227 neuraminidase activity of the NA was not necessary for the release of NA-VLP in cells (Fig.
228 5).

229

230 To characterize the NA-VLPs, biochemical, physical, morphological and functional
231 studies were done, including sucrose gradient flotation profile, NA functional assay, detection
232 of multimeric NA, TEM study, as well as desialylation of surface sialic acid on the cells
233 producing NA-VLPs. The presence of both influenza virions and NA-VLPs in the middle
234 fractions of the sucrose gradient (Fig. 3a and b-d) indicates that VLPs have a buoyant
235 density equivalent to native influenza viruses. The enzymatic activity assay showed that NAs
236 on the particle surface were functionally active and the activity was in proportion to the
237 amount of protein (Fig. 3f). The morphology of the VLPs was found to resemble influenza
238 virions. Most of the VLP were spherical although elongated particles were also detected (Fig.
239 2b & 2f). No morphological difference was observed in NA-VLPs from high pathogenic avian
240 influenza H5N1, seasonal H1N1, and pandemic swine-origin H1N1 (Supplementary data S1).

241

242 It is conceivable that exosomes or vesicles arising from apoptotic bodies may be
243 mistaken as VLPs. However, electron microscopy failed to reveal either apoptosis or the
244 formation of intracellular vesicles (such as the multivesicular bodies of exosomes).
245 Furthermore, we also monitored for apoptosis in transfected cells by attempting to

246 demonstrate the expression and cleavage of caspase-3 in the course of the experiment. Only
247 the uncleaved form of caspase-3 could be detected for the first 60 hours post-transfection
248 suggesting that VLP-producer cells were not undergoing apoptosis (Fig. 4b). Cross-sections
249 of membrane protrusions such as filopodia (Fig. 2a, arrowhead B) do occur and these may
250 be mistaken as budding of VLP. However, they can be distinguished from the “typical VLP”
251 by electron microscopy because VLPs (Fig. 2a, arrowhead A) have a more electron dense
252 outline which is distinguishable from the cell membrane, except at the budding sites of virus
253 or VLPs (Fig. 2). Taken together, these data indicate that the particles observed in the EM
254 are true viral like particles.

255

256 NAs on the particle surface were found to be tetrameric in the influenza virions, which
257 is important for some of the NA functions. Using the cross-linker DTSSP, multimeric NA were
258 protected from urea and we were able to detect NA multimeric complexes comparable to that
259 found on fully infectious H1N1 virions. This result was expected as maturation of the NA has
260 been described to take place in the endoplasmic reticulum (ER) where the NA-tetramers
261 form before going through the Golgi network to the assembly site at the plasma membrane
262 (Saito et al., 1995). Therefore, budding of the NA-VLPs (or virus) from the cell surface will be
263 expected to incorporate only mature tetrameric NA proteins with similar oligomerization as
264 would the influenza virus. Failure to detect NA from virions after DTSSP treatment may be
265 caused by conformational changes of the protein upon conjugation. The cross-linker may
266 also modify or hide the residues (such as lysine) involved in the antibody binding site. Our
267 data indicated that NA on the VLP surface was in oligomeric form although the technique
268 used did not allow us to quantify the ratio between the monomer, dimer, trimer and tetramer
269 (Fig. 6).

270

271 All three neuraminidases included in the study were able to cleave cell surface sialic
272 acids in both α -2,3 and α -2,6 linkage. As the technique used is qualitative rather than
273 quantitative, we could not quantify a preference in the cleavage activity to sialic acid with α -

274 2,3 linkage (Supplementary data S2), as mentioned in previous findings using H1N1 and
275 H3N2 virus NA (Mochalova *et al.*, 2007; Franca de Barros *et al.*, 2003). We detected a
276 significant increase of β -Gal-GalNAc in NA-expressing cells by the PNA binding. This
277 supports the role of NA enzymatic activity during the initial stage of infection by helping the
278 virus to penetrate through the mucus layer where sialic acid is mainly linked to Gal-GalNAc in
279 α -2,3 configuration.

280

281 Neuraminidase is an important viral component of influenza viruses and the most
282 effective anti-influenza drugs in the market are NA inhibitors. Although NA has been studied
283 for decades, most of the data were obtained from purified virion which requires access to a
284 high bio-containment laboratory when dealing with highly pathogenic avian influenza viruses.
285 Purified NA proteins were also widely used for NA study but these isolated NA may not have
286 the same properties as NA on viral surface. It was in fact reported that substrate specificities
287 of sialidase activity from purified NA and their original viruses were not identical (Nagai *et al.*,
288 1995). NA-VLPs produced in our study, though non-infectious, were multivalent, antigenic,
289 enzymatically active and morphologically similar to native influenza viruses. Therefore they
290 could be a preferable alternative to recombinant NA peptides or proteins as immunogen to
291 produce antibodies against neuraminidase or as antigens for ELISA type assays. In addition,
292 because NAs on the VLPs surface were not only functionally active but also presented in
293 multimeric form, these VLPs are a useful tool to investigate NA interactions with the host
294 cells, as well as neuraminidase inhibitor drugs.

295

296 **Methods**

297 **Plasmids.** Plasmids pcDNA-HA, pcDNA-NA(H5), and pcDNA-M1 respectively
298 corresponding to DNA sequences of HA (GI:126361929), NA (GI: 126361907) from influenza
299 A/Cambodia/JP52a/2005 (H5N1) and M1 (GI: 81975893) from influenza
300 A/Goose/Guangdong/1/96 (H5N1) were cloned into the mammalian expression vector
301 pcDNA3.1 (Invitrogen). Both non-tagged and FLAG-tagged HA and NA proteins in the C-

302 terminus were used. For the study of neuraminidase from different viral subtypes, plasmids
303 pcDNA-NA(H1) and pcDNA-NA(pdmH1) encoding the FLAG-tagged NA of influenza
304 A/Gansu/Chenguan/1129/2007 (seasonal H1N1; GI:194140557) and A/California/04/2009
305 (swine origin pandemic H1N1; GI:227977118) were prepared respectively. Enzymatically
306 inactive pcDNA-NA(E262D) was prepared from pcDNA-NA(H5) by point mutation using
307 QuikChange® II Site-Directed Mutagenesis Kit (Stratagene) according to manufacturer's
308 instructions and post-sequencing selection of clones based on NA-Star chemoluminescent
309 assay (Applied Biosystems).

310

311 **Cells and viruses.** HEK-293T and MDCK cells were grown in Dulbecco's modified
312 Eagle's medium (DMEM) supplemented with 10 % fetal bovine serum (FBS) and 1 %
313 penicillin-streptomycin at 37 °C with 5 % CO₂. Influenza A/WSN/33 (H1N1) virus was
314 propagated in MDCK cells with culture medium supplemented with 0.5 µg.mL⁻¹ TPCK-treated
315 trypsin. Highly pathogenic avian influenza (HPAI) A/Hong Kong/483/97 H5N1 virus was
316 propagated in MDCK in MEM culture medium.

317

318 **Antibodies and Western blotting.** Vaccinated chicken sera containing anti-HA
319 antibodies (haemagglutination inhibition titer >256) and polyclonal antibodies from rabbit
320 hyper-immunized with avian Influenza A neuraminidase (Abcam) were used to detect non-
321 tagged HA and NA proteins respectively. Anti-FLAG monoclonal mouse antibody (Sigma)
322 was used to detect FLAG-tagged HA and NA. Monoclonal mouse antibody GA2B (Abcam)
323 was used for the detection of influenza M1 protein. For western blotting, samples were
324 resolved in 4-12 % SDS-PAGE (Invitrogen), electroblotted to polyvinylidene fluoride
325 transfer membrane, hybridized with appropriate antibodies and detected with ECL Western
326 Detection Reagent (Amersham). Protein size was estimated using the Novex® Sharp Pre-
327 stained Protein Standard (Invitrogen). The fraction of protein released in supernatant (SN)
328 was expressed as a percentage of overall expressed protein both in lysates and in SN
329 adjusted to the respective volumes followed by normalization relative to GAPDH

330 housekeeping protein expression detected with anti-GAPDH Mouse Monoclonal (6C5)
331 antibody (Abcam). Quantification was performed by densitometry on scanned images
332 obtained using Scion Image Beta 4.0.3 (Scion Corporation). Each quantification was
333 associated with a calibration curve using a range of BAP-flag protein (Sigma) covering the
334 range of concentration measured. The exposure times were chosen in order to quantify the
335 signal intensity within the linear range of the calibration curve below saturation of the signal
336 as monitored by the image analysis.

337

338 **Detection of VLP production in cells expressing influenza HA, NA and M1**
339 **proteins.** HEK-293T cells were transfected with different combinations of plasmids using
340 CalPhos Mammalian Transfection Kit (Clontech) according to the manufacturer's instructions.
341 The amount of plasmids pcDNA-HA, pcDNA-NA(H5) and pcDNA-M1 in the transfection
342 mixture was 5 µg each, and empty vector was used to replace the omitted plasmids when
343 appropriate. At 12 hours post-transfection, the medium was replaced with fresh DMEM-10%
344 FBS, and exogenous bacterial neuraminidase (*Vibrio cholerae*, Roche; 6.25 mU.mL⁻¹) was
345 added to the medium when appropriate. At 60 hours post-transfection, supernatant was
346 collected and cell debris were removed by filtration through 0.45 µm filters. Filtered culture
347 medium was then layered onto a 30 % sucrose-HEPES buffer (2 mM HEPES, 125 mM NaCl,
348 0.9 mM CaCl₂, 0.5 mM MgCl₂, pH 7.4) cushion and centrifuged at 28,000 rpm for 2.5 hours at
349 4 °C and the pellet was resuspended in HEPES buffer. Cell lysates were collected at the
350 same time by the addition of lysis buffer (20 mM Tris-HCl, 1 mM EDTA, 150 mM NaCl, 0.1 %
351 SDS, 1 % Triton-X, protease inhibitor mixture (Roche Diagnostics) followed by centrifugation
352 at 13,000 rpm for 10 minutes. Samples were mixed with 4X LDS sample buffer (Invitrogen)
353 and dithiothreitol (DTT, 100 mM), boiled for 8 minutes and analyzed by western blotting as
354 described above.

355

356 **H5N1 virion preparation and analysis.** MDCK cells, plated the day before, were
357 inoculated for 1 h at 37 °C with H5N1 virus at multiplicity of infection of 1. After washing with

358 phosphate buffer saline (PBS), infected cells were incubated at 37 °C overnight. Twenty
359 hours post-infection, the supernatant was harvested, clarified by centrifugation before
360 concentration on 100 kDa pore filter Amicon system (Millipore) and finally resuspended in
361 lysis buffer (50 mM KCl, 1 % NP-40, 25 mM HEPES (pH 7.4), 1 mM DTT, protease inhibitor
362 mixture (Roche Diagnostics)). Cell lysates were also collected after addition of lysis buffer to
363 the infected cells. In each sample, loading buffer (prepared from 6X: 62.5 mM Tris-HCl (pH
364 6.8), 25 % Glycerol, 2 % SDS, 0.01 % bromophenol blue, 5 % β-mercaptoethanol) was
365 added, boiled for 10 minutes so they can be taken out from the biosafety level 3 laboratory
366 (BSL-3).

367

368 **NA-VLP and H1N1 virion preparation and analysis.** For NA-VLP production, HEK-
369 293T, HeLa, and A549 cells were transfected with 10 µg of pcDNA-NA(H5), pcDNA-NA(H1)
370 or pcDNA-NA(pdmH1) as indicated above. Transfection with equal amount of empty vector
371 was carried out as a mock control. After ultracentrifugation of clarified supernatant (as
372 described above), the pellet was resuspended in NTE (100 mM NaCl, 10 mM Tris (pH 7.4), 1
373 mM EDTA), put onto a sucrose gradient (20-60 %) and centrifuged at 35,000 rpm for 2 hours
374 at 4 °C. Twenty fractions were manually collected from the top to bottom.

375

376 Influenza A/WSN/33 (H1N1) virions were purified from infected MDCK cultures at 72
377 hours post-infection. The supernatant was harvested and clarified by centrifugation at 4,000
378 rpm for 15 min. Virions were then pelleted, put onto sucrose gradient (20-60 %) and
379 centrifuged as described above for VLPs. Recombinant NA proteins purified from transfected
380 cell lysates by immunoprecipitation using anti-FLAG M2-agarose affinity gel (Sigma), were
381 layered onto sucrose gradient as above, as additional control.

382

383 All the upper-mentioned sucrose fractions of VLPs, virions and purified proteins were
384 boiled in LDS loading buffer with DTT, and analyzed by western blotting (see above).
385 Sialidase activities of the NA-VLPs and purified proteins were measured by NA-Star

386 chemoluminescent assay (Applied Biosystems). Oligomerization of NA on the VLP surface
387 was studied using the cross-linker 3,3'-dithio-bis(sulfosuccinimidylpropionate) (DTSSP,
388 Thermo Scientific). NA-VLPs were mixed with DTSSP (5 mM) to stabilize the multimeric NA
389 complexes, prior to the addition of LDS loading buffer followed by addition of urea (8 M) or
390 DTT (100 mM) when appropriate. DTSSP pre-treated VLPs were directly analyzed by
391 western blotting as described above.

392

393 **Electron microscopy (EM).** Transfected HEK-293T cells were fixed with 2.5 %
394 glutaraldehyde in 0.1 M cacodylate buffer (pH 7.4) and post-fixed with 1 % osmium tetroxide.
395 The fixed cells were then pelleted in 1 % agar, dehydrated in increasing concentration of
396 ethanol, and embedded in epoxy resin. Ultra-thin sections of the samples were visualized
397 with Philips EM208s electron microscope after staining with 2 % aqueous uranyl acetate and
398 Reynold's lead citrate.

399

400 **Kinetics of NA-VLP release.** HEK-293T cells were transfected with pcDNA-NA(H5)
401 or pcDNA-NA(pdM1) as mentioned above. At 12 hours post-transfection, the culture
402 medium was replaced with fresh DMEM-10% FBS. Supernatant and cell lysates were
403 collected at 20, 28, 36 and 60 hours post-transfection as described above. Samples were
404 boiled with LDS loading buffer and DTT for 8 minutes and were analyzed by western blotting.

405

406 **Effect of neuraminidase enzymatic activities on production of VLP.** A single
407 amino acid change E262D in the NA is known to abrogate the sialidase activity of the NA
408 molecule (Huang et al., 2008). HEK-293T cells were transfected with pcDNA-NA(H5) or
409 pcDNA-NA(E262D), with or without pcDNA-HA. At 12 hours post-transfection, the culture
410 media were refreshed and sialidase inhibitor (Oseltamivir carboxylate, 50 μ M) was added to
411 the medium as indicated. Supernatant and cell lysates were collected at 60 hours post-
412 transfection and protein levels in VLPs were analyzed by western blotting. Sialidase activities

413 of the supernatant were measured by NA-Star chemoluminescent assay (Applied
414 Biosystems).

415

416 **Lectin staining for cells surface sialic acid.** Lectin histochemistry analysis was
417 performed as previously described (Nicholls *et al.*, 2007). Briefly, HEK-293T cell lines stably
418 or transiently expressing N1 from seasonal H1N1 (HuN1) or pandemic H1N1 (pdmN1) or
419 avian influenza H5N1 (AvN1) were fixed with 4 % paraformaldehyde (PFA). After washing
420 with PBS, lectin staining was performed with *Sambucus Nigra* agglutinin (SNA-I, Roche) and
421 *Maackia amurensis* agglutinin (MAA-II, Vector) to detect α -2,6 or α -2,3 linked sialic acid (SA)
422 respectively. Peanut agglutinin (PNA, Roche) was used to identify the terminal Gal-GalNAc.
423 Biotin conjugated lectins were used with avidin-peroxidase counterstaining (Vector).

424

425 **Acknowledgements**

426 This work was supported by the Area of Excellence Scheme of the University Grants
427 Committee (grant AoE/M-12/-06 of the Hong Kong Special Administrative Region, China),
428 the University Grants Committee project HKU 10208924 and HKU 4774109, the French
429 Ministry of Health, RESPARI Pasteur network and the Li Ka Shing Foundation. We would like
430 to thank Dr K. Y. Hui (Department of Microbiology, the University of Hong Kong) for carrying
431 out the bio-safety level-3 work on H5N1.

432

433 **References**

434 **Air, G.M. & Laver, W.G. (1989).** The neuraminidase of influenza virus. *Proteins* **6**, 341-356.

435

436 **Barman, S., Adhikary, L., Chakraborti, A.K., Bernas, C., Kawaoka, Y. & Nayak, D.P.**
437 **(2004).** Role of transmembrane domain and cytoplasmic tail amino acid sequences of
438 influenza A virus neuraminidase in raft-association and virus budding. *J Virol* **78**, 5258-69.

439

440 **Bucher, D. & Palese, P. (1975).** The biologically active proteins of influenza virus:

441 neuraminidase. In *The influenza viruses and influenza*, pp. 83-123
442 Edited by E Kilbourne, Academic Press, New York.

443

444 **Chen, B.J., Leser, G.P., Morita, E. & Lamb, R.A. (2007).** Influenza virus hemagglutinin and
445 neuraminidase, but not the matrix protein, are required for assembly and budding of plasmid-
446 derived virus-like particles. *J Virol* **81**, 7111-23.

447

448 **França de Barros, J. Jr., Sales Alviano, D., da Silva, M.H., Dutra Wigg, M., Sales**
449 **Alviano, C., Schauer, R. & dos Santos Silva Couceiro, J.N. (2003).** Characterization of
450 sialidase from an influenza A (H3N2) virus strain: kinetic parameters and substrate specificity.
451 *Intervirology* **46**, 199-206.

452

453 **Fujiyoshi, Y., Kume, N.P., Sakata, K. & Sato, S.B. (1994).** Fine structure of influenza A
454 virus observed by electron cryo-microscopy. *EMBO J* **13**, 318-26.

455

456 **Gómez-Puertas, P., Albo, C., Perez-Pastrana, E., Vivo, A. & Portela, A. (2000).** Influenza
457 virus matrix protein is the major driving force in virus budding. *J Virol* **74**, 11538-47.

458

459 **Huang, I.C., Li, W., Sui, J., Marasco, W., Choe, H. & Farzan, M. (2008).** Influenza A virus
460 neuraminidase limits viral superinfection. *J Virol.* **82**, 4834-43.

461

462 **Jin, H., Leser, G.P., Zhang, J. & Lamb, R.A. (1997).** Influenza virus hemagglutinin and
463 neuraminidase cytoplasmic tails control particles shape. *EMBO J* **16**, 1236-47.

464

465 **Latham, T. & Galaeza, J.M. (2001).** Formation of wild-type and chimeric influenza virus-like
466 particles following simultaneous expression of only four structural proteins. *J Virol* **75**, 6154-
467 65.

468

469 **Liu, C., Eichelberger, M.C., Compans, R.W. & Air, G.M. (1995).** Influenza type A virus
470 neuraminidase does not play a role in viral entry, replication, assembly, or budding. *J Virol* **69**,
471 1099-106.

472

473 **Matrosovich, M.N., Klenk, H.D. & Kawaoka, Y. (2006).** Receptor specificity, host range and
474 pathogenicity of influenza viruses. In *Influenza virology: current topics*, pp 95-137. Edited by
475 Y Kawaoka, Caister Academic Press, Wymondham, England.

476

477 **Matrosovich, M.N., Matrosovich, T.Y., Gray, T., Roberts, N.A. & Klenk, H.D. (2004).**
478 Neuraminidase is important for the initiation of influenza virus infection in human airway
479 epithelium. *J Virol* **78**, 12665-7.

480

481 **Mochalova, L., Kurova, V., Shtyrya, Y., Korchagina, E., Gambaryan, A., Belyanchikov, I.**
482 **& Bovin, N. (2007).** Oligosaccharide specificity of influenza H1N1 virus neuraminidases.
483 *Arch Virol* **152**, 2047-57.

484

485 **Nagai, T., Suzuki, Y. & Yamada, H. (1995).** Comparison of substrate specificities of
486 sialidase activity between purified enzymes from influenza virus A (H1N1 and H3N2
487 subtypes) and B strains and their original viruses. *Biol Pharm Bull* **18**, 1251-1254.

488

489 **Nayak, D.P., Balogun, R.A., Yamada, H., Zhou, Z.H. & Barman, S. (2009).** Influenza virus
490 morphogenesis and budding. *Virus Research* **143**, 147-61.

491

492 **Neumann, G., Watanabe, T. & Kawaoka, Y. (2000).** Plasmid-driven formation of influenza
493 virus-like-particles. *J Virol* **74**, 547-551.

494

495 **Nicholls, J.M., Bourne, A.J., Chen, H., Guan, Y. & Peiris, J.S. (2007).** Sialic acid receptor
496 detection in the human respiratory tract: evidence for widespread distribution of potential
497 binding sites for human and avian influenza viruses. *Respir Res* **8**, 73.

498

499 **Noda, T., Sagara, H., Yen, A., Takada, A., Kida, K., Cheng, R.H. & Kawaoka, Y. (2006).**
500 Architecture of ribonucleoprotein complexes in influenza A virus particles. *Nature* **439**, 490-
501 492.

502

503 **Ohuchi, M., Asaoka, N., Sakai, T. & Ohuchi, R. (2006).** Roles of neuraminidase in the initial
504 stage of influenza virus infection. *Microbes Infect* **8**, 1287-93.

505

506 **Saito, T., Taylor, G. & Webster, R.G. (1995).** Steps in maturation of influenza A virus
507 neuraminidase. *J Virol* **69**, 5011-7.

508

509 **Shaw, M.L., Stone, K.L., Colangelo, C.M., Gulcicek, E.E. & Palese, P. (2008).** Cellular
510 proteins in influenza virus particles. *PLoS Pathog* **4**, e1000085.

511

512 **Su, B., Wurtzer, S., Rameix-Welti, M.A., Dwyer, D., van der Werf, S., Naffakh, N., Clavel,
513 F. & Labrosse, B. (2009).** Enhancement of the influenza A hemagglutinin (HA)-mediated
514 cell-cell fusion and virus entry by the viral neuraminidase (NA). *PLoS One* **4**, e8495.

515

516 **Tscherne, D.M., Manicassamy, B. & Garcia-Sastre, A. (2010).** An enzymatic virus-like
517 particle assay for sensitive detection of virus entry. *J Virol Methods* **163**, 336-43.

518

519 **Wang, D., Harmon, A., Jin, J., Francis, D.H., Christopher-Hennings, J., Nelson, E.,
520 Montelaro, R.C. & Li, F. (2010).** The Lack of an Inherent Membrane Targeting Signal is
521 Responsible for the Failure of the Matrix (M1) Protein of Influenza A Virus to Bud into Virus-
522 Like-Particles. *J Virol* **84**, 4673-81.

523

524 **Zhang, J., Pekosz, A. & Lamb, R.A. (2000).** Influenza virus assembly and lipid raft
525 microdomains: a role for the cytoplasmic tails of the spike glycoproteins. *J Virol* **74**, 4634-44.

526

527 **Figures legends:**

528

529 **Figure 1. Detection of viral proteins from transfected HEK-293T cells.** (a) Evaluation of
530 the contribution of different viral structural proteins HA, NA, and M1 from H5N1 expressed in
531 HEK-293T cells in combinations as indicated and comparison with H5N1 whole virus (b).
532 Exogenous bacterial NA (exoNA) was added to the medium when indicated. VLPs released
533 in the culture medium were harvested at 60 hr post-transfection and pelleted through a 30 %
534 sucrose cushion. Samples were analyzed by SDS-PAGE followed by immunoblotting to
535 detect different viral proteins together with the lysates of transfected cells. Percentages of
536 protein released were calculated as fraction detected in the supernatant from the overall
537 protein detected both in lysates (Lys) and supernatants (SN). Apparent sizes of the HA, M1
538 and NA were ~27 kDa (HA2), ~28 kDa and ~55 kDa respectively.

539

540 **Figure 2. Transmission Electron Microscopy of cells expressing HA, NA and M1 from**
541 **A/Cambodia/JP52a/2005 (H5N1).** HEK-293T cells were processed for electron microscopy
542 at 36 h post-transfection. VLP budding was observed in cell expressing HA without
543 exogenous NA treatment (a & b) or with the addition of exogenous NA (c) or when NA was
544 expressed alone (d & f), but not when M1 was expressed alone. (e). Arrowheads : A: VLP; B:
545 filopodia.

546

547 **Figure 3. Physical and functional characterization of NA-VLPs.** Western blot analysis of
548 fractions from sucrose gradient from 20 % (fraction 1) to 60 % (fraction 20) sucrose of
549 A/WSN/33 (H1N1) virions collected from infected MDCK cells (a), from supernatant of HEK-
550 293T cells transfected with NA plasmid from seasonal H1N1 (b), pandemic H1N1 (c), HPAI
551 H5N1 (d) or from immuno-purified N1 protein (e). Neuraminidase enzymatic activity of the
552 corresponding sucrose fractions were tested with NA-Star chemoluminescent assay (f) and
553 expressed in arbitrary unit (AU) defined as the percentage of the fraction with the highest
554 signal.

555

556 **Figure 4. Kinetics of N1-VLP release.** (a) Neuraminidase enzymatic activity (expressed in
557 relative luminescence unit, RLU) from the supernatant of HEK-293T cells transfected with NA
558 from either pandemic H1N1 (plain line) or H5N1 (broken line) tested with NA-Star
559 chemoluminescent assay. Experiment performed in triplicate. (b) Evaluation of percentage of
560 NA released by western blot analysis of supernatant and transfected cell lysates; and
561 monitoring of Caspase-3 cleavage (uncleaved (#) and cleaved (*) forms). The percentage of
562 release was calculated as indicated in Methods section. Lysate from H5N1 virus-infected
563 cells was used as positive control (Ctl) for cleaved form of caspase-3.

564

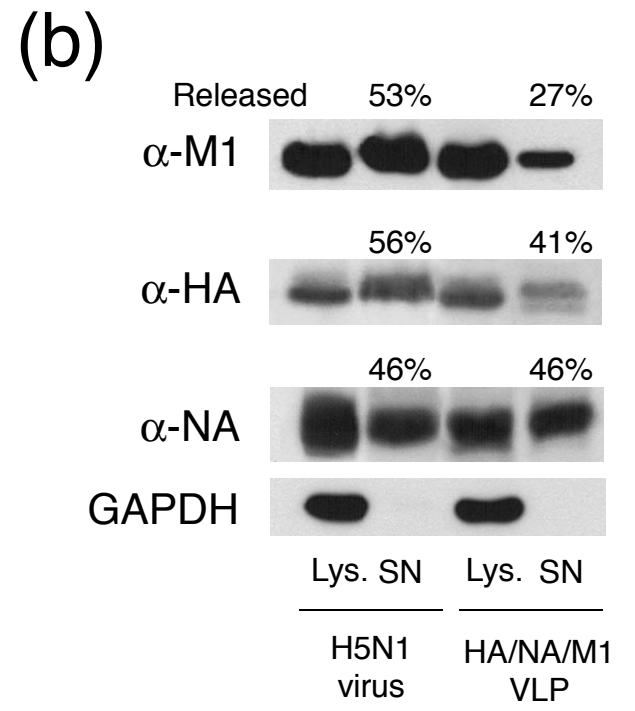
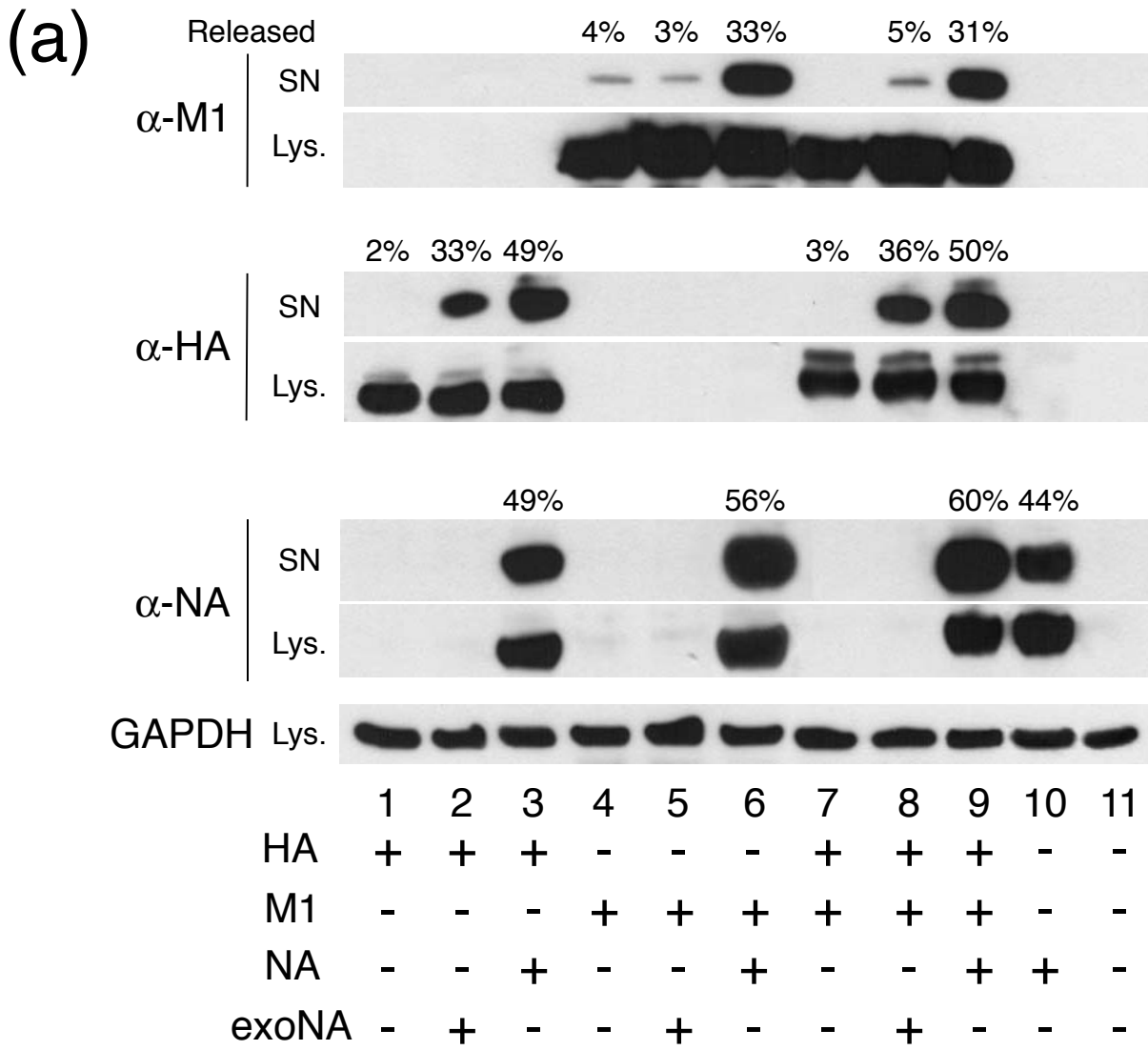
565 **Figure 5. Influence of NA sialidase activity on NA-VLP release.** Neuraminidase
566 enzymatic activity (expressed in relative luminescence unit, RLU) from the supernatant of
567 HEK-293T cells transfected with NA (either from H5N1 wild-type (wt), or with mutation
568 E262D (mut)) alone or co-expressed with HA; in absence or presence of Oseltamivir (OsIt).
569 Evaluation of percentage of NA released by western blot analysis of supernatant (SN) and
570 transfected cell lysates (Lys) (2X). Percentage of NA release was calculated as indicated in
571 Methods section. Bkg: background level.

572

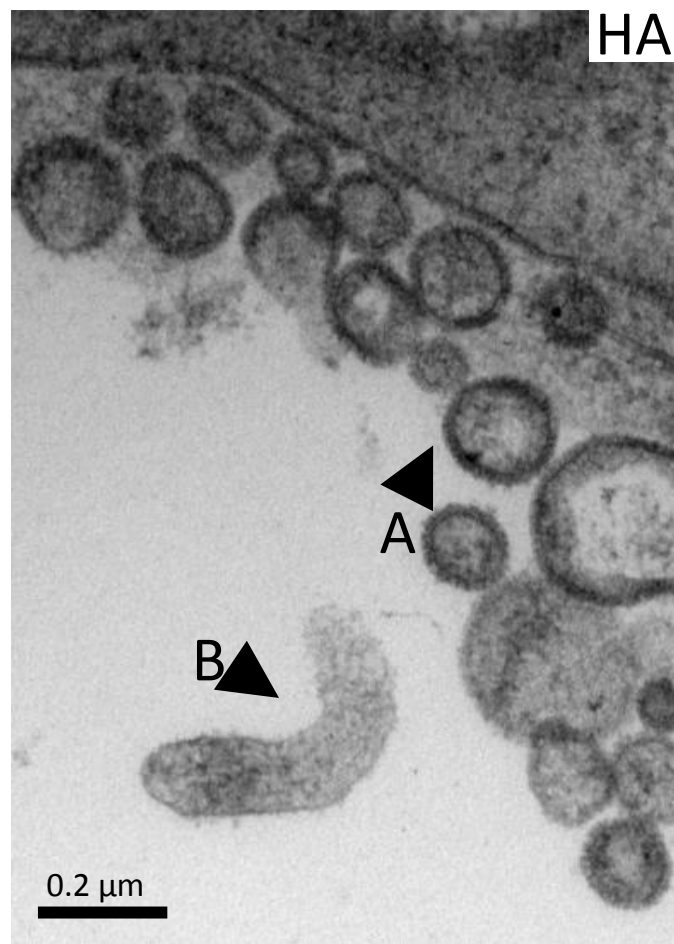
573 **Figure 6. Detection of multimeric NA complexes on VLPs.** N1-VLPs were resolved in 4-
574 12 % SDS-PAGE after heating in SDS loading buffer (lane 1), and with the addition of urea
575 or DTT (lanes 2 and 3 respectively). Similar treatments were done on NA-VLPs pre-treated
576 with cross-linker DTSSP (lanes 4 to 6). Samples from SDS-PAGE were then transfer to
577 PVDF membrane and immunoblotted with monoclonal anti-FLAG antibodies. H1N1 virions
578 were included for comparison and NA were detected using anti-NA antibodies. Apparent
579 sizes of NA monomer, dimer, trimer and tetramer were ~55 kDa, ~110 kDa, ~165 kDa, and
580 ~220 kDa respectively.

581

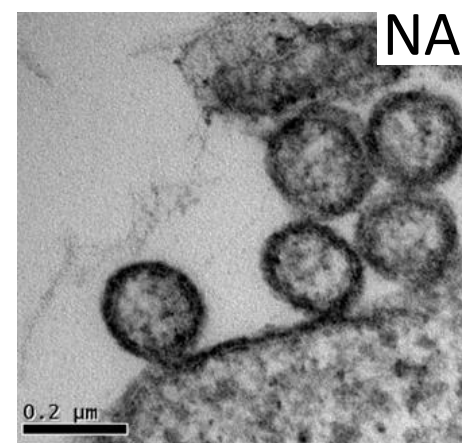
582



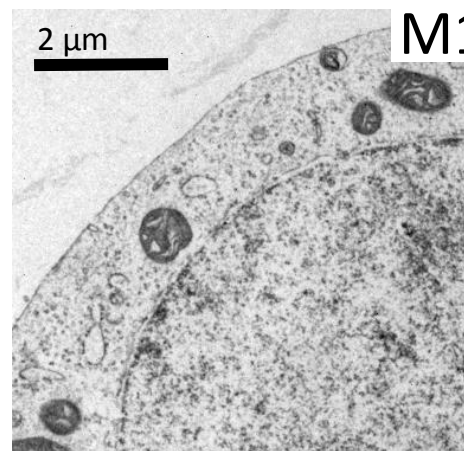
(a)



HA (b)



NA (d)

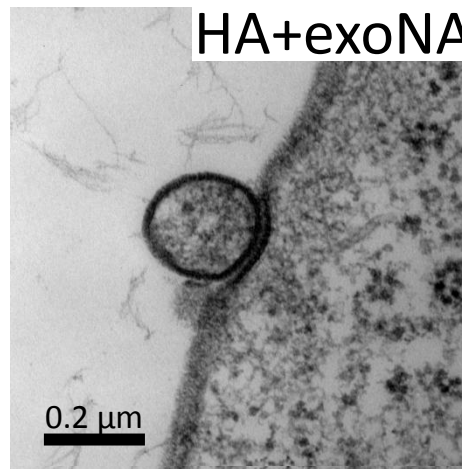


(f)

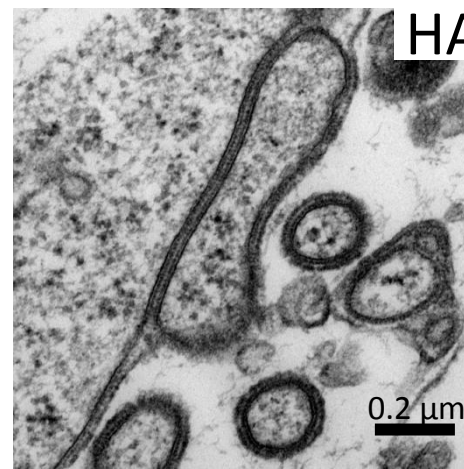


NA

(c)

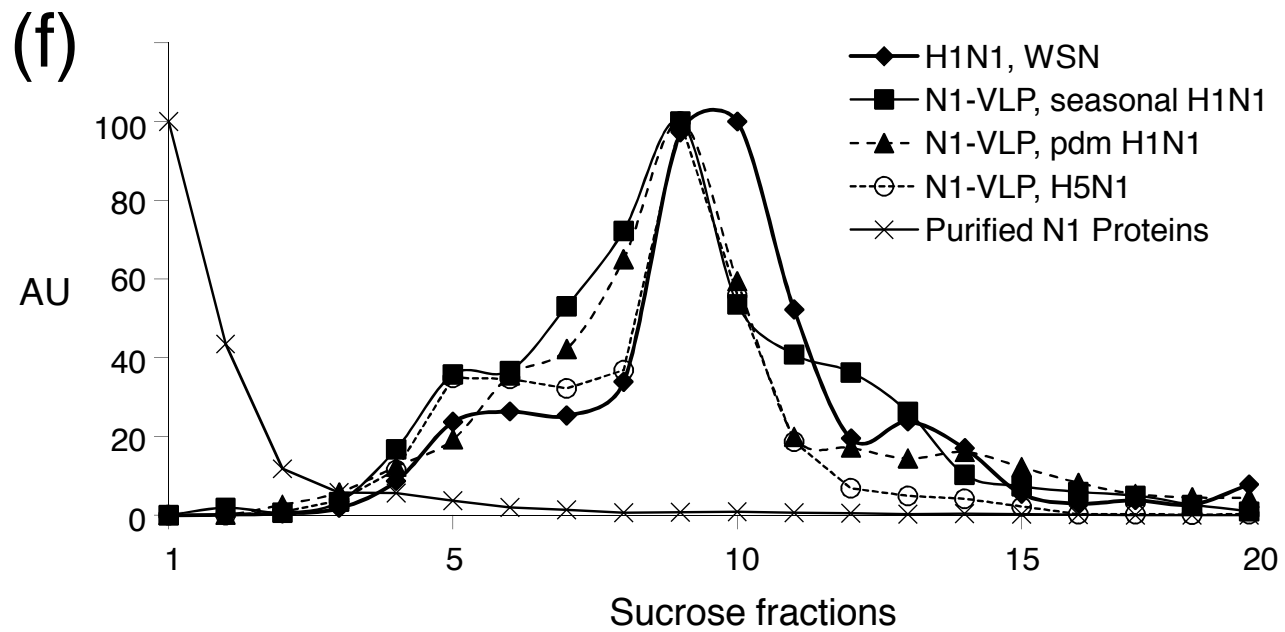
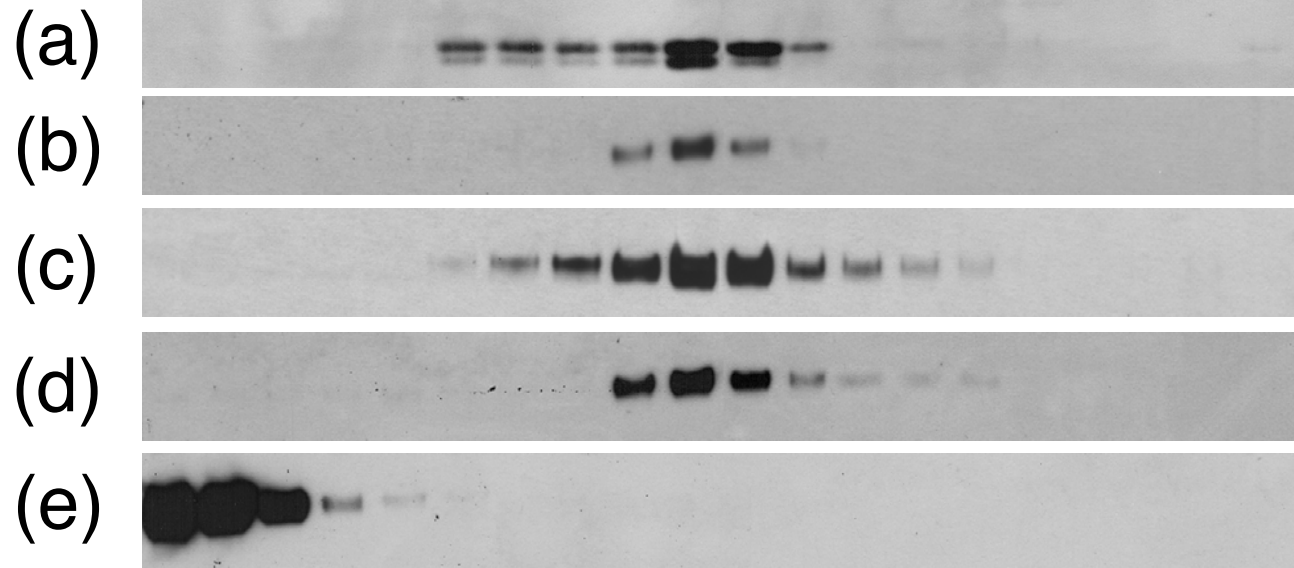


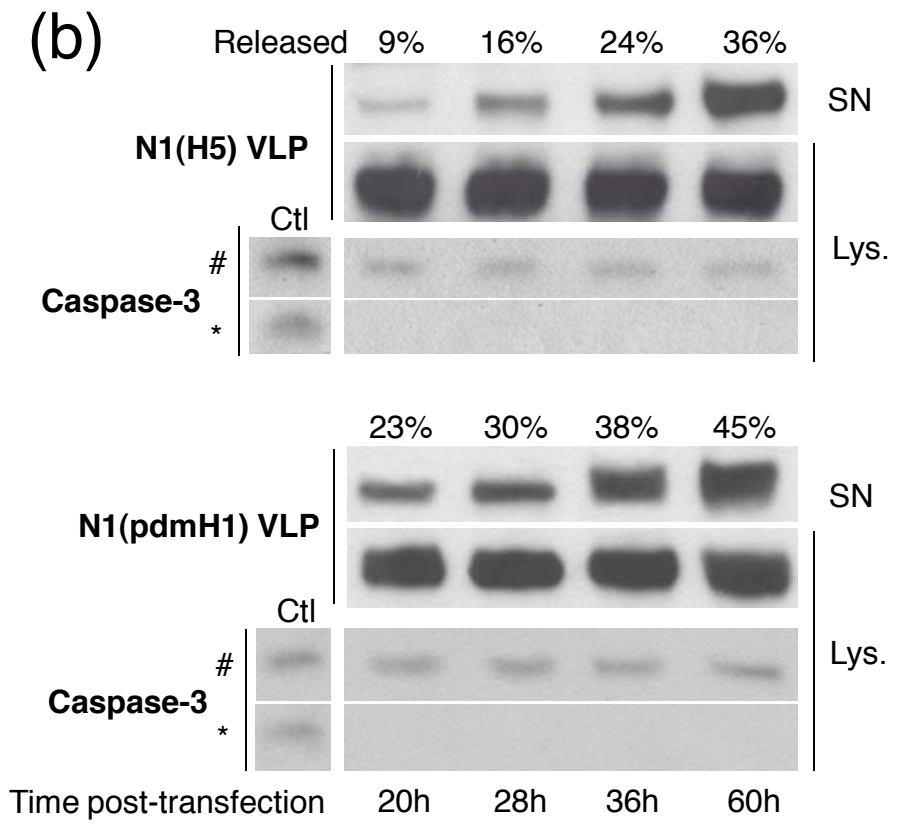
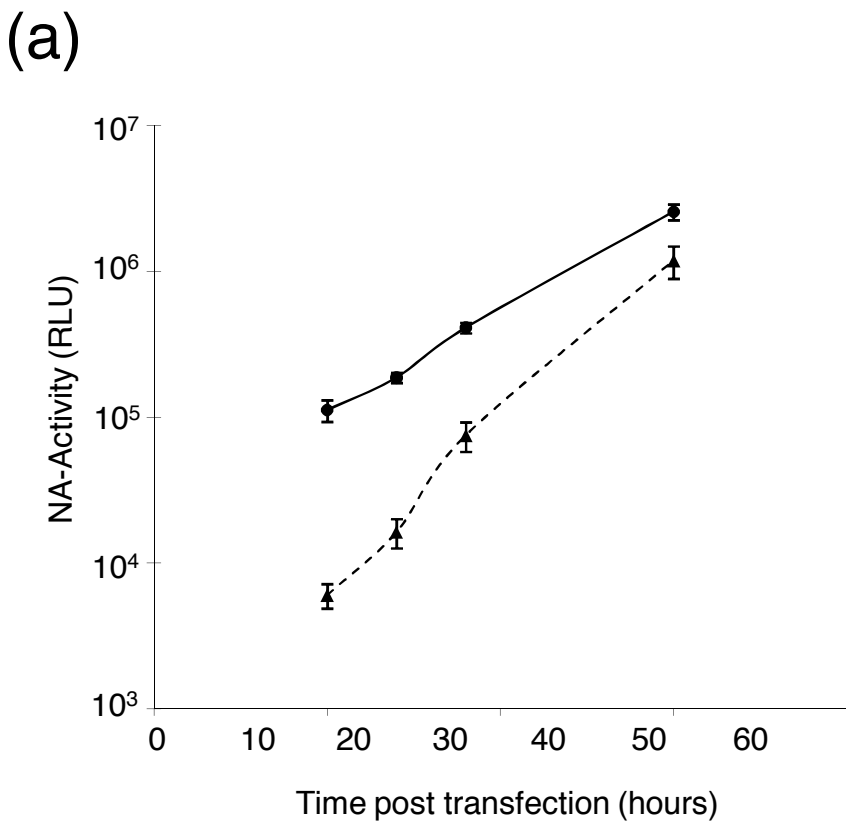
HA+exoNA (e)

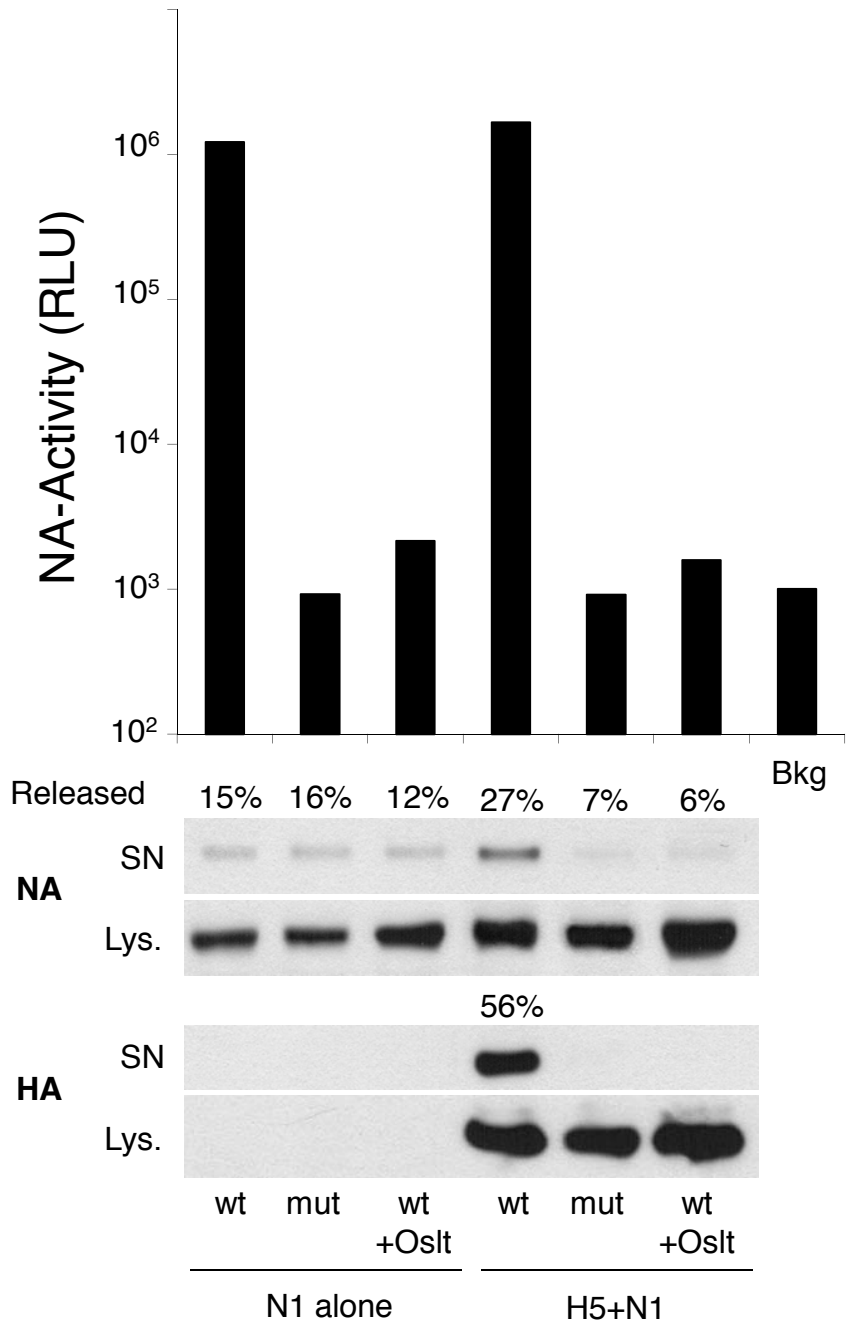


HA

20% ————— Sucrose Gradient —————> 60 %







| | | | | | | | | |
|-------|---|---|---|---|---|---|---|---|
| SDS | + | + | + | + | + | + | + | + |
| Urea | - | + | - | - | + | - | - | - |
| DTT | - | - | + | - | - | + | - | - |
| DTSSP | - | - | - | + | + | + | - | + |

